DEMANDE D'AUTORISATION N°
EN VUE D'UNE PUBLICATION OU D'UNE COMMUNICATION

Direction : ....DTA.....
Centre : ....FAR .....
Réf émetteur : .STR/95-32 ..

NIG n° 316

DL529/N. FR9503429

Titre original du document : PASSIVE HYBRID FORCE-POSITION CONTROL FOR TELEOPERATION BASED ON REAL-TIME SIMULATION OF A VIRTUAL MECHANISM

Titre traduit en anglais :

Titre traduit en français : COMMANDE HYBRIDE FORCE-POSITIVE PASSIVE POUR LA TELEOPERATION BASEE SUR LA SIMULATION EN TEMPS REEL D'UN MECANISME VIRTUEL

AUTEURS	AFFILIATION [1]	DEPT/SERV/SECT	VISA (d'un des auteurs)	DATE
JOLY L.	CEA	DTA/STR/LAC		08.01.95
ANDRIOT C.	CEA	DTA/STR/LAC		

Nature du document [2] :

PERIODIQUE	CONF/CONGRÈS	POSTER	RAPPORT	THÈSE	COURS	MÉMOIRE DE STAGE	Chapitre d'OUVRAGE
☐	☒	☐	☐	☐	☐	☐	☐

Pièces jointes : RÉSUMÉ ☐ TEXTE ☒

CONGRES / CONFERENCE : Nom : 7th INTERNATIONAL CONFERENCE ON ADVANCED ROBOTICS (ICAR'95)
Ville : Sant Feliu de Guixols, Pays : Espagne Date du : 20/09/95 au : 22/09/95

Organisateur : Universitat Politecnica de Catalunya

PERIODIQUE : Titre :
Comité de lecture : oui ☐ non ☐

OUVRAGE : Titre :
Éditeur :

THESE / MEMOIRE DE STAGE / COURS : Université / Établissement d'enseignement :

DOMAINES : |__|__|__|__|

LANGUE : ANGLAIS

N° EPAC : |__|__|__|__|

SUPPORT : Disquette ☐ Papier ☒

MOTS-CLES : Téléopération, commande hybride force-position, commande passive, suivi de surface.

Les visas portés ci-dessous attestent que la qualité scientifique et technique de la publication proposée a été vérifiée et que la présente publication ne divulgue pas d'information brevetable, commercialement utilisable ou classée.

	SIGLE	NOM	DATE	VISA	OBSERVATIONS	REF
CHEF DE SERVICE	STR	J.M.DETRICHE	11/1/95		favorable -	
CHEF DE DEPARTEMENT	DPSA	A.GOUFFON	12/1/95		favorable.	

1 modif.

Date limite d'envoi du résumé : Date limite d'envoi du texte : 15/01/95 limite d'envoi du poster :.../.../...

Destinataires:
Les correspondants publication des départements se chargent de transmettre à l'INSTN/MIST/CIRST (Saclay) copies des demandes d'autorisation de publication, du résumé et du texte définitif.

[1] Entité d'appartenance de l'auteur. Ex. : CEA, CNRS, INSERM ...
[2] Cocher la case correspondante

We regret that some of the pages in this report may not be up to the proper legibility standards, even though the best possible copy was used for scanning

Passive Hybrid Force-Position Control for Teleoperation Based on Real-Time Simulation of a Virtual Mechanism

Luc D. JOLY and Claude ANDRIOT
Commissariat à l'Energie Atomique (CEA/CERET)
Service de Téléopération et Robotique
BP 6, Route du Panorama
92265 FONTENAY-AUX-ROSES, FRANCE
tandriot@suisse.far.cea.fr

Abstract: *Hybrid force-position control aims at controlling position and force in separate directions. It is particularly useful to perform certain robotic tasks. In teleoperation context, passivity is important because it ensures stability when the system interacts with any passive environement. In this paper, we propose an original approach to hybrid force-position control of a force reflecting telerobot system. It is based on real-time simulation of a virtual mechanism corresponding to the task. The resulting control law is passive. Experiments on a 6 degrees of freedom teleoperation system consisting in following a bended pipe under several control modes validate the approach.*

keywords : teleoperation, hybrid force-position control, passive controller, surface following

INTRODUCTION

The work reported here is part of the TAO 2000 project currently under development at CEA. This project is concerned with the realisation of a computer-aided teleoperation system for nuclear applications.

The control of manipulator during contact tasks involves the control of interaction forces. This has been the subject of a great amount of research work [1]. Most approches can be grouped into two main classes: *hybrid force/position control* (or hybrid control) and *impedance control*.

Hybrid control has been introduced by Raibert and Craig [2]. Many improvements have been added to the original scheme (e.g. [3],[4],[5]) but the basic idea has remained unchanged. The task space is splitted into force controlled and position controlled directions ([6]) in which two separate controllers operate. Independance of the controllers is obtained by means of projection operators (e.g. selection matrices).

On the other hand, the aim of impedance control [7] is not to control separately force and position in distinct directions, but rather the relationship between force and motion. The manipulator is intended to veer away from the desired trajectory according to the forces exerted on it.

Most impedance control laws have been designed so that the robot impedance at the contact port be passive. This ensures coupled stability when the manipulator interacts with any passive environment. But the fact that interaction forces cannot be controlled can be considered to be a drawback of this approach. Conversely, most hybrid control schemes were not shown to be passive. (See [8], [9] for counter-examples.)

In teleoperation, bilateral position-position coupling can be related to impedance control. A relation between the position error and the torques sent to the master and slave arms is implemented. This results in a passive behavior of the system. Passivity is all the more important since the environment is usually unstructured. Introducing position or force commands in some directions and controlling them using selection matrices often destroys the passivity property.

An easy strategy to ensure passivity of the controlled system is to design a controller mimicking the behavior of a physical (passive) system interacting with the master and slave arms. Hybrid control can be achieved by simulating an ideal virtual mechanism linked to the master and slave arms by springs and dampers (impedance control). This idea is a generalisation of [10] which presented a controller designed to impose motion constraints to a teleoperation system. The virtual mechanism constitutes a global parametrisation of the task. Some of its joints are position controlled, whereas the others are force controlled. It describes the ideal behavior that should have the system during the task execution. The real arms will behave as desired if the spings and dampers are sufficiently stiff.

The paper is organised as follows. After a few preliminaries (Section 1), we derive the control law (Section 2). An example shows how a virtual mechanism can be designed to perform a hybrid task (Section 3). Finally, we describe and give the results of an experiment consisting in following a bended pipe using several control modes (Sections 4 and 5).

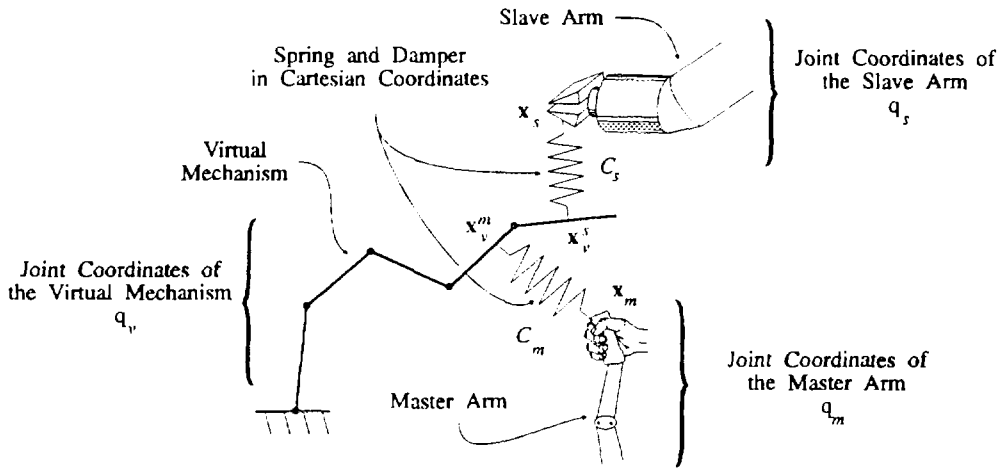

Fig. 1: The concept of virtual mechanism.

1. PRELIMINARIES

Throughout the paper, the subscripts *m*, *s* and *v* stand respectively for master arm, slave arm and virtual mechanism. The subscipt *i* replaces either *m* or *s*.

1.1. The master and slave arms

We suppose the master and slave arms are rigid, backdriveable and have respectively n_m and n_s degree of freedom (DOF). Due to high-gear ratio the slave arm is often not backdriveable. In this case, sensitivity to external forces can be achieved by closing a local force loop around the arm [7].

Notice the arms may have distinct geometry and different number of DOF. Their joint positions and velocities are assumed to be measured and are represented respectively by $\mathbf{q}_m, \dot{\mathbf{q}}_m \in \mathbf{R}^{n_m}$ and $\mathbf{q}_s, \dot{\mathbf{q}}_s \in \mathbf{R}^{n_s}$.

The letter $\mathbf{p}$ will denote Cartesian positions. The master and slave positions are respectively mapped into two cartesian spaces C_m and C_s, by the forward kinematics:

$$\mathbf{p}_i = \mathrm{K}_i(\mathbf{q}_i) \in C_i \quad (i = m \text{ or } s)$$

These functions include possibly indexing and size scaling. To avoid representation singularities, we have defined Cartesian orientations with Euler parameters (normalised quaternions) ([11], for example).

Let the letter $\mathbf{v}$ denotes vectors representing Cartesian velocities. The master and slave Cartesian velocities are related to the corresponding joint velocities by the jacobian matrices:

$$\mathbf{v}_i = \mathbf{J}_i(\mathbf{q}_i)\dot{\mathbf{q}}_i \quad (i = m \text{ or } s)$$

1.2. The virtual mechanism

We consider a n_v DOF virtual mechanism with n_p position controlled joints and n_f force controlled joints ($n_v = n_p + n_f$). Its joint position and velocity are defined by the vectors $\mathbf{q}_v, \dot{\mathbf{q}}_v \in \mathbf{R}^{n_v}$. These vectors can be splitted in force controlled. and position controlled coordinates:

$$\mathbf{q}_v = \left[\mathbf{q}_v^{p\,t}, \mathbf{q}_v^{f\,t}\right]^t \text{ and } \dot{\mathbf{q}}_v = \left[\dot{\mathbf{q}}_v^{p\,t}, \dot{\mathbf{q}}_v^{f\,t}\right]^t$$

It constitutes a "natural" parametrisation of the task. This will be more obvious in the example. $\mathbf{q}_p(t)$ and $\dot{\mathbf{q}}_p(t)$ are known functions of time.

To each joint position of the virtual mechanism, we associate two Cartesian positions in C_m and C_s, respectively.

$$\mathbf{p}_v^i = \mathrm{K}_v^i(\mathbf{q}_v) \in C_i \quad (i = m \text{ or } s)$$

These positions represent the point of the virtual mechanism which will be linked to arm *i* by a spring and a damper (Fig. 1).

The associated Cartesian velocities are:

$$\mathbf{v}_v^i = \mathbf{J}_v^i(\mathbf{q}_v)\dot{\mathbf{q}}_v \quad (i = m \text{ or } s)$$

These vectors are the sum of two terms, corresponding to the position and force controlled joint velocities:

$$\mathbf{v}_v^i \triangleq \mathbf{v}_p^i + \mathbf{v}_f^i \triangleq \mathbf{J}_p^i(\mathbf{q}_v)\dot{\mathbf{q}}_p + \mathbf{J}_f^i(\mathbf{q}_v)\dot{\mathbf{q}}_f \quad (i = m \text{ or } s) \tag{1}$$

We assume that the virtual mechanism has been chosen such that one of the matrices $\mathbf{J}_f^i$ has full row rank (i.e. $\mathrm{rk}\left(\mathbf{J}_f^i\right) = n_f$, for $i = m$ or s).

Let $\mathbf{f}$ denote Cartesian forces and $\boldsymbol{\tau}$ generalised joint forces. Let $\mathbf{f}_v^i$ be the force exerted on the virtual mechanism at the point $\mathbf{p}_v^i$. Since the virtual mechanism

is ideal -no mass, no damping- the joint driving forces τ_v exactly compensate for the external forces. Then:

$$\tau_v + \left(\mathbf{J}_v^m\right)^t . \mathbf{f}_v^m + \left(\mathbf{J}_v^s\right)^t . \mathbf{f}_v^s = \mathbf{0}_{n_v \times 1} \quad (2)$$

The part of this vector corresponding to force controlled joints is:

$$\tau_f + \left(\mathbf{J}_f^m\right)^t . \mathbf{f}_v^m + \left(\mathbf{J}_f^s\right)^t . \mathbf{f}_v^s = \mathbf{0}_{n_f \times 1} \quad (3)$$

where $\tau_f(t)$ is a known function of time.

2. CONTROL LAW

The control law is obtained by simulating the virtual mechanism attached to the master and slave arms by generalised springs and dampers defined in Cartesian coordinates. First, we will establish the ordinary differential equation (ODE) which rules the motion of the virtual mechanism. This will enable us to compute the driving torques to be sent to the master and slave arms. Finally, we will give the algorithm we have used for digital implementation.

2.1. ODE ruling the virtual mechanism motion

The force $\mathbf{f}_v^i$ results of the action of the spring and damper connecting the arm i and the virtual mechanism:

$$\mathbf{f}_v^i = \mathbf{f}_{sp,v}^i(\mathbf{p}_i, \mathbf{p}_v^i) + \mathbf{B}_i(\mathbf{v}_i - \mathbf{v}_v^i) \quad (i = m \text{ or } s) \quad (4)$$

where $\mathbf{B}_i \in \mathbf{R}^{6\times 6}$ is a symmetric positive definite matrix.

Conversely, the force exerted at the arm i tip is:

$$\mathbf{f}_i = \mathbf{f}_{sp,i}(\mathbf{p}_i, \mathbf{p}_v^i) - \mathbf{B}_i(\mathbf{v}_i - \mathbf{v}_v^i) \quad (i = m \text{ or } s) \quad (5)$$

To represent the action of a spring, the repelling forces $\mathbf{f}_{sp,v}^i$ and $\mathbf{f}_{sp,i}$ exerted at both extremities of the generalised spring must derive from a potential energy, i.e. they must satisfy:

$$\mathbf{v}_i^t . \mathbf{f}_{sp,i} + \mathbf{v}_v^{i\,t} . \mathbf{f}_{sp,v}^i = -\frac{dE_{pot,i}}{dt} \quad (i = m \text{ or } s) \quad (6)$$

The repelling linear force we have used is proportionnal to position error, and the repelling torque is parallel to the rotation error axis, and proportional to $\sin(\Delta\theta/2)$, where $\Delta\theta$ is the rotation error angle. The associated potential energy is given in [8].

Substituting (1) and (4) in (3), one can easily obtain:

$$\dot{\mathbf{q}}_v = \left(\sum_{i=m,s} \left(\mathbf{J}_f^i\right)^t . \mathbf{B}_i . \mathbf{J}_f^i \right)^{-1} \cdot \left(\sum_{i=m,s} \left(\mathbf{J}_f^i\right)^t . \left(\mathbf{f}_{sp,v}^i(\mathbf{p}_i, \mathbf{p}_v^i) + \mathbf{B}_i . (\mathbf{v}_i - \mathbf{v}_f^i)\right) + \tau_f \right) \quad (7)$$

The matrix to be inverted is symmetric, positive definite due to the rank assumption of paragraph 1.2. If the initial value of $\mathbf{q}_v$ is given, this ODE can be integrated in real-time, using the known values of $\mathbf{q}_p$, $\dot{\mathbf{q}}_p$, and τ_f, and the measured values of $\mathbf{p}_i$ and $\mathbf{v}_i$.

2.2. Master and slave driving torques

Once the whole position and velocity of the virtual mechanism is known, the driving torques may be calculated by:

$$\begin{cases} \tau_m = \lambda . \mathbf{J}_m^t \mathbf{f}_m \\ \tau_s = \mathbf{J}_s^t \mathbf{f}_s \end{cases} \quad (8)$$

with $\mathbf{f}_i$ given by (5).

The scalar $\lambda > 0$ is introduced to scale the forces reflected to the master. It has been showed that it does not affect coupled stability properties ([8],[12]).

2.3. Digital implementation

Digital implementation can be done with the following cyclic algorithm:

1- Measure the slave and master states. The virtual mechanism state $\mathbf{q}_v$ results from the previous time step (or is given at the first step).
2- Compute the virtual mechanism velocity in the force controlled directions by (7).
3- Compute the master and slave joint driving torques using (8).
4- Integrate the (7) by a numerical method over the time step to compute the next position of the virtual mechanism.

Remark: Numerical integration has been done by the explicit Euler scheme with one integration step per control cycle. This method is not the most precise, but has the advantage of requiring little computation. No stability problems have been encountered, as long as the jacobians of the virtual mechanism were continuous. Otherwise, limit cycles could occur near discontinuity because (7) had no static solution.

2.4. Passivity of the controller

Since all the equations writen in the control law describe physical systems interacting with each other, the controller is obviously passive. The interested reader may be conviced by computing the integral of the power flow entering the controller. A few algebraic manipulations that we will no detail give:

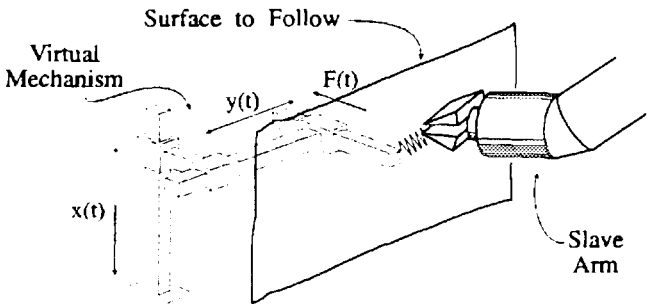

Fig. 2: Using a virtual mechanism for surface following

$$\int_0^t (\dot{q}_m^t \cdot \tau_m + \dot{q}_s^t \cdot \tau_s + \dot{q}_v^t \cdot \tau_v)\, dt$$

$$= \sum_{i=m,s} E_{pot,i}(t) - \sum_{i=m,s} E_{pot,i}(0) + \int_0^t \sum_{i=m,s} (\mathbf{v}_i - \mathbf{v}_v^i)^t \mathbf{B}_i (\mathbf{v}_i - \mathbf{v}_v^i)\, dt$$

$$\geq - \sum_{i=m,s} E_{pot,i}(0) = -\gamma^2$$

The power entering the controller is either stored in the springs or dissipated.

3. EXAMPLE

In this section, we will give an example to show how the concept of vitual mechanism can be used to do hybrid control. To simplify we first consider the case of an autonomous mode of operation, that is the master arm is not connected to the virtual mechanism. The control equations remain unchanged, excepted the sums " $\sum_{i=m,s}$ " in which term corresponding to the master arm dissapear.

A typical task for which hybrid control is suited consists in moving a tool on an approximatively plane surface while exerting a given normal effort on it. The virtual mechanism suited for this application is shown on Fig. 2. The first two DOF are position controlled. They specify the trajectory in the plane. The last DOF is force controlled. It gives compliance to the system in the direction in wich the robot has to adapt its trajectory to the surface.

One can note that the virtual mechanism fits geometrically to the task. It has the same number of DOF and its joints coordinates describe the task in a natural way. The virtual mechanism can then be considered as (one of) the ideal robot designed to perform a given task.

4. EXPERIMENT DESCRIPTION

4.1. The telerobotic system

Experiments were performed on a telerobotic systems consisting of a MA23 master arm and a RD500 slave arm, both having 6 electrically-powered DOF. The RD500 is a dismantling robot with 50 kg payload capacity. Each of its joints is equiped with a force sensor around which a local force loop is closed (P.D.). The MA23 is backdriveable.

For safety reasons, the digitally implemented controller runs in parallel on two C30 microprocessors - one for each arm - exchanging data through serial communication. The servo rate is around 300 Hz.

Due to the difference between the arms strengths, the force scaling factor $\lambda = 0.1$ has been used in each experiment.

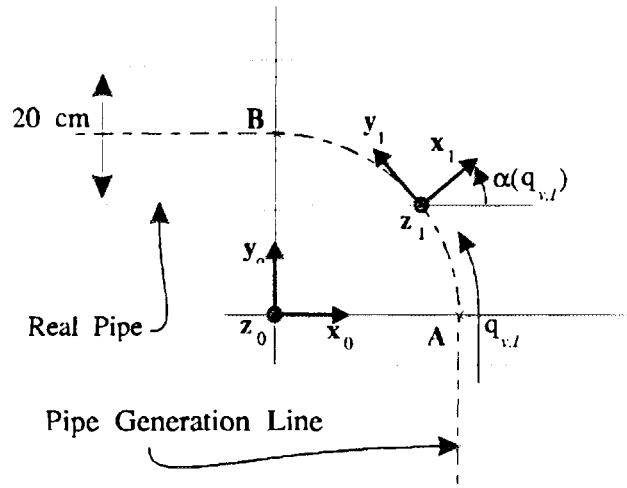

Fig. 3: The first DOF of the virtual mechanism

4.2. Decontamination task

The experiments presented here were suggested by a typical task in nuclear teleoperation. Decontamination of surfaces can be carried out by scrubbing. This task involves moving a scrubbing tool normally along the surface while applying a constant force. The surfaces to be decontamined are usually complex.

The experiment consisted in following a bended pipe with a hard plastic ball (representing the scrubbing tool) fixed on the slave end effector. The bended pipe used can be approximately described by two cylinders (Ø 20 cm) connected by a torus part (90° bend, radius 20 cm).

This task is rather difficult. The operator must keep the tool perpendicular to the complex surface while applying a roughly constant normal force, all this without direct vision. We will show how the proposed approach permits to derive several control modes which make the task much easier.

4.3. The virtual mechanism

The virtual mechanism has been chosen to fit to the task geometry. It has four DOF: three to describe the position (and orientation) on the surface, and one to deal with the contact force. Its position in the robot workspace is given by the frame R_0.

The first DOF combines a translation along the pipe generation curve and a rotation aroud z_0 (Fig. 3). The

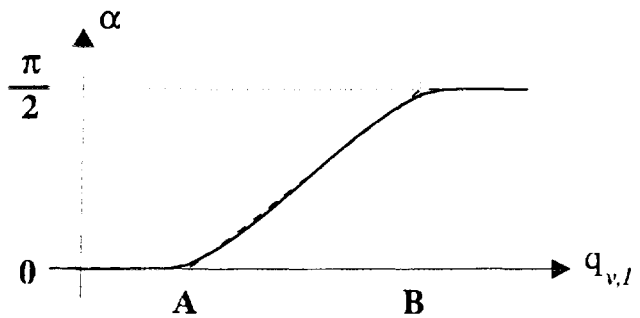

Fig. 4: orientation of the frame R_1. dashed: piecewice linear; solid: polynomial approximation.

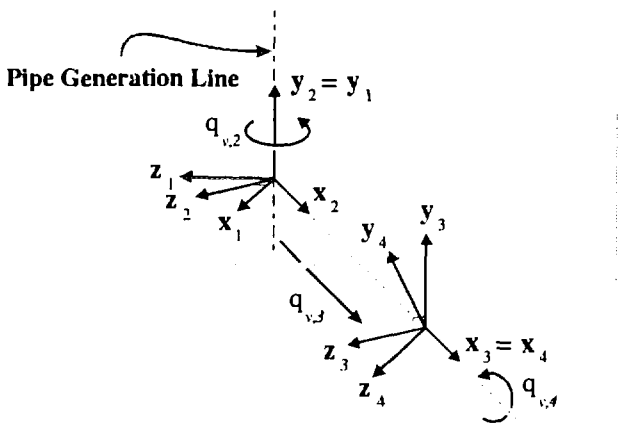

Fig. 5: The last three DOF of the virtual mechanism used for pipe following.

rotation angle α depends on the curvilinear abscissa $q_{v,1}$. If the axis $\mathbf{y}_1$ is tangent to the pipe generation line, then $\alpha(q_{v,1})$ is piecewise linear. Consequently, its derivative is not continuous at points A and B. To have a continuous derivative, $\alpha(q_{v,1})$ has been approximated by a third degree polynomial (Fig. 4). The resulting lack of accuracy is of no importance compared to the irregularitiess on the real pipe (joins, fastening straps,...).

The three other DOF are as follows (Fig. 5). $q_{v,2}$ defines the rotation around axis $\mathbf{y}_1$. The translation along $\mathbf{x}_2$ is parametrised by $q_{v,3}$. Finally, $q_{v,4}$ is the rotation angle around $\mathbf{x}_3$.

5. EXPERIMENTAL RESULTS

In this section, we compare the task execution under different control modes.

5.1. Full manual mode

It is quite difficult for rather untrained operators (the authors) to execute the task properly in manual mode (only indirect vision and force feedback). Contact is often lost and the orientation of the tool is inacurate (Fig. 6) The average orientation error is 20° (angle between the end effector and the direction normal to the surface).

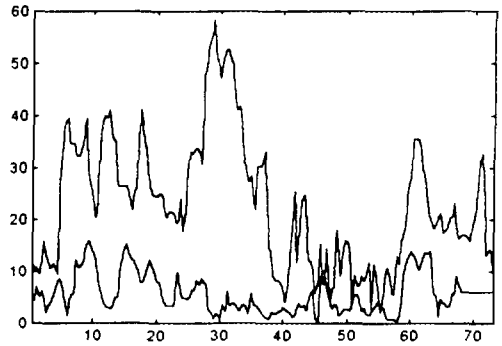

Fig. 6: slave orientation error (degrees) versus time (seconds) during manipulation. dashed: full manual mode; solid: constrained mode

5.2. Kinematic constraint

In this control mode, the virtual mechanism is force controlled, with all desired forces equal to zero. The slave and master end-effectors are both "connected" to the extremity of the virtual mechanism. In this case, the virtual mechanism behaves as a kinematic constraint acting on the teleoperation system. The telerobot workspace is virtually reduced to the four degrees of freedom of the virtual mechanism. The tool is then automatically constrained to remain orthogonal to the pipe surface.

The operator is then releived of a part of the task. This results in more safety and quality. This assistance appeared to be very helpful. Contact losses were very seldom and orientation error was reduced to approximatively 5° (Fig. 6). The remaining orientation error is caused by contact friction forces.

5.3. Automatic normal force

In the previous case, the operator had to exert a constant pressure on the master arm to maintain contact. To avoid this, a desired force has been added on the third DOF of the virtul mechanism, ie the normal direction. The value needed to maintain contact was about 90 N, which corresponds to 9 N for the operator (Recall the force scaling factor $\lambda = 0.1$). The force exerted on the master by the operator in the normal direction is added to the nominal force.

The contact force is better controlled than in the previous case. It is easily adapted when the ball moves over irregularities on the pipe. The RD500 has no end-effector force sensor, so this assumption is only qualitative.

5.4. Quasi-automatic mode

In this control mode, $K_v^m(.)$ and $K_v^s(.)$ are different. Of course, the associated jacobians also differ. $K_v^s(.)$ corresponds to the forward kinematics of the virtual

mechanism presented previously. The third DOF (normal direction) is force controlled, wheras the three others are position controlled. On the master side, $K_v^m(.)$ depends only on the force controlled parameter. It corresponds to a translation along an arbitrary straight line.

When this control mode is activated, the slave arm describes a path on the pipe. The master arm is automatically constrained on a line. When the operator pushes on it, the slave increases the normal contact force and he or she feels it back. Conversely, pulling on the master makes the slave move away from the pipe. Moreover, if the operator tries to drive the master away from the line, he or she feels a repelling force, but this does not disturb the slave motion.

Unidirectional force feedback was sufficiently accurate to feel the normal motion when the tool passed over irregularities. This control mode was the one which made the task easiest.

CONCLUSION

Based on physical analogy, we have designed a passive hybrid force-position controller for teleoperation application. It mimics the action of a mechanical system connected to the master and slave arms by springs and dampers.

Despite it has been designed to achieve hybrid control, full position control or full manual control (with force feedback) can be done. They correspond to the two "degenerated" cases were the virtual mecanism has 6 DOF and is totally position controlled or respectively totally force controlled with desired force equal to zero. This unified view results in a very modular overall controller. Each operation mode corresponds to a specific virtual mechanism.

Experimental results presented in this paper show that the approach is valid and can be used to create a wide range of fonctionnalities. Of course, complex surface following is not the single application and has been presented here as an example.

Another advantage of the "mechanical equivalence" of the controller is that it can easily be programmed through a graphical interface. Some present work at CEA deals with the coupling of this controller with trajectory generator, telerobotic programming language, graphical programming interface, computer-aided environment modelling and geometrical data basis.

REFERENCES

[1] D. E. Whitney, *Historical Perspective and State of the Art in Robot Force Control*, International Journal of Robotics Research, vol. 6, no. 1, pp. 3-14, 1987.

[2] M. H. Raibert, J. J. Craig, *Hybrid Position/Force Control of Manipulators*, Journal of Dynamic systems, Measurement and Control, vol. 102, pp. 126-133, 1981.

[3] O. Khatib, *A Unified Approach for Motion and Force Control of Robot Manipulators*, IEEE Journal of Robotics and Automation, vol. 3, pp. 43-53, 1987.

[4] T. Yoshikawa, *Dynamic Hybrid Position/Force Control of Robot Manipulators - Description of Hand Constraints and Calculation of Joint Driving Torques*, IEEE Journal of Robotics and Automation, vol. 3, pp. 386-392, 1987.

[5] A. De Luca, C. Manes,...

[6] M. T. Mason, *Compliance and Force Control for Computed Controlled Manipulators*, IEEE Transactions on Systems, Man, and Cybernetics, SMC-11, pp. 418-432, 1981.

[7] Neville Hogan, *Impedance Control: An Approach to Manipulation*, ASME Journal of Dynamic Systems and Control, Vol. 107, pp. 1-24, 1985.

[8] R. J. Anderson, *A Network Approach to Force Contol in Robotics and Teleoperation*, Ph.D. thesis, University of Illinois at Urbana-Champaign.

[9] Suguru Arimoto, *State-of-the-Art and Future Research Directions of Robot Control*, Proceedings of the Fourth IFAC Symposium on Robot Control, pp. 3-14, September 19-21, Capri, Italy, 1994.

[10] L. D. Joly, C. Andriot, *Imposing Motion Constraints to a Force-Reflective Telerobot through Real-Time Simulation of a Virtual Mechanism*, submitted to IEEE International Conference on Robotics and Automation, may 1995, Nagoya, Japan.

[11] C. Samson, M. Le Borgne, B. Espiau, *Robot Control, The Task Function Approach*, Oxford University Press, 1990.

[12] J. E. Colgate, *Power and Impedance Scaling in Bilateral Manipulation*, Proceedings of the 1991 International Conf. on Robotics and Automation, Sacramento, CA, April 1991.